

Computational Fluid Dynamics 2004

C. Groth · D. W. Zingg (Editors)

Computational Fluid Dynamics 2004

Proceedings
of the Third International Conference
on Computational Fluid Dynamics, ICCFD3,
Toronto, 12–16 July 2004

With 627 Figures and 47 Tables

 Springer

Professor Clinton Groth
Professor David W. Zingg

University of Toronto
Institute of Aerospace Studies
Dufferin Street 4925
M3H 5T6 Downsview, Ontario
Canada

e-mail: groth@utias.utoronto.ca
dwz@oddjob.utias.utoronto.ca

Library of Congress Control Number: 2006928440

ISBN-10 3-540-31800-3 Springer Berlin Heidelberg New York

ISBN-13 978-3-540-31800-2 Springer Berlin Heidelberg New York

This work is subject to copyright. All rights are reserved, whether the whole or part of the material is concerned, specifically the rights of translation, reprinting, reuse of illustrations, recitation, broadcasting, reproduction on microfilm or in any other way, and storage in data banks. Duplication of this publication or parts thereof is permitted only under the provisions of the German Copyright Law of September 9, 1965, in its current version, and permission for use must always be obtained from Springer. Violations are liable for prosecution under the German Copyright Law.

Springer is a part of Springer Science+Business Media

springer.com

© Springer-Verlag Berlin Heidelberg 2006
Printed in Germany

The use of general descriptive names, registered names, trademarks, etc. in this publication does not imply, even in the absence of a specific statement, that such names are exempt from the relevant protective laws and regulations and therefore free for general use.

Typesetting by the editors, final processing by LE-TeX GbR, Leipzig
Production: LE-TeX Jelonek, Schmidt & Vöckler GbR, Leipzig
Cover design: *design & production*, Heidelberg

Printed on acid-free paper 54/3100/YL 5 4 3 2 1 0

Preface

This book contains the Proceedings of the Third International Conference on Computational Fluid Dynamics (ICCFD), held in Toronto, Ontario, Canada from July 12 through 16, 2004. The ICCFD series has evolved into the leading international conference series for scientists, mathematicians, and engineers interested in the computation of fluid flow. Invited keynote lectures were given by renowned researchers in the areas of detached-eddy simulation, micro-flow simulations, control of shocks, multiscale models of the circulatory system, and high-end computing in aerospace.

Abstracts were received from 23 countries. The executive committee, consisting of C. Bruneau, J.-J. Chattot, D. Kwak, N. Satofuka, K. Srinivas, and myself, was responsible for selection of papers. Each of the members had a separate subcommittee to carry out the evaluation. As a result of this careful peer review process, 123 papers were selected for oral presentation and a further 67 for poster presentation. The conference was attended by 172 delegates from 22 different countries.

Thanks are due to our sponsors, NASA and the Institute for Aerospace Research of the National Research Council of Canada. In particular, the generous grant from NASA is a key factor in the success of this conference series. I would also like to thank the staff at the Westin Harbour Castle, all who participated in the organization of the conference, including the review process, and the students of the CFD group at the University of Toronto Institute for Aerospace Studies for the tremendous help they provided toward the success of this conference.

These Proceedings contain a snapshot of the field of computational fluid dynamics as of 2004. They present a vibrant field with strong capabilities in many areas of application and a myriad of opportunities for future contributions to science and engineering.

Toronto, Canada
September 2004

David W. Zingg
Conference Chair

Contents

Part I Invited Lectures

Topics in Detached-Eddy Simulation

Philippe R. Spalart 3

High-End Computing Challenges in Aerospace Design and Engineering

F. Ronald Bailey 13

Control of Shocks in CFD

Claude Bardos, Olivier Pironneau 27

A Domain Decomposition Framework for Fluid-Structure Interaction Problems

Simone Deparis, Marco Discacciati, Alfio Quarteroni 41

Micro Flow Simulation Using Kinetic and Continuum Approaches

Koji Morinishi 59

Part II Acoustics

A Hybrid FE/Spectral Analysis of Turbofan Aeroacoustics

M. C. Duta, M. B. Giles, A. Laird 77

Numerical Simulation of the Oscillations in a Mixer - An Internal Aeroacoustic Feedback System

Philip C. E. Jorgenson, Ching Y. Loh 83

CFD Simulations of Acoustic Wave Phenomena in Combustion Chambers

Venkateswaran Sankaran, Guoping Xia, Matthew Ellis, Charles Merkle 89

Computation on Wake/Stator Interaction in a 2D Cascade

X.Y. Wang, A. Himansu, S.C. Chang, P. Jorgenson 95

Part III Adaptive Meshing

An Error Indicator for Semidiscrete Schemes <i>Daniele Marobin, Gabriella Puppo</i>	103
A Mesh Adjustment Scheme for Embedded Boundaries <i>J. S. Sachdev, C. P. T. Groth</i>	109
Numerical Simulations of Flows Past 2D Complex Shapes Using Building Cube Method <i>Siro Kitamura, Yoshinori Inoue, Takehisa Iwai</i>	115
High-Density Mesh Flow Computations by Building-Cube Method <i>Kazuhiro Nakahashi, LaeSung Kim</i>	121

Part IV Algorithms

A Matrix-Free Implicit Method for Flows at All Speeds <i>Alberto Beccantini, Christophe Corre, Thibaud Kloczko</i>	129
An Efficient and Accurate Pressure-Correction Method for All Mach Numbers <i>Krista Nerinckx, Jan Vierendeels, Erik Dick</i>	135
The Analysis of Electromagnetic Waves Using CIP Scheme with Soroban Grid <i>Yoichi Ogata, Takashi Yabe, Kenji Takizawa, Tomomasa Ohkubo</i>	141
Multigrid Third-Order Least-Squares Solution of Cauchy-Riemann Equations on Unstructured Triangular Grids <i>Hiroaki Nishikawa</i>	147
Solution of the Fluid Dynamical Formulation of Nonlinear Schrödinger Equation with Radial Basis Function Interpolation <i>T. Y. Hsieh, J. C. Huang, J. Y. Yang</i>	153
High Resolution Schemes for Quantum Hydrodynamics Based on Nonlinear Schrödinger Equation <i>J. Y. Yang, J. C. Huang, T. Y. Hsieh</i>	159
Multigrid Acceleration for Transonic Aerodynamic Flow Simulations Based on a Hierarchical Formulation <i>Mohamed Hafez, Essam Wahba</i>	165

A New Accurate and Stable Least-Square Method to Compute the Gradient on Non-Orthogonal Meshes
Céline Béchaud, Khalid Yagobi, Frédéric Archambeau, Namane Méchitoua 171

Robustness of a Characteristic Finite Element Scheme of Second Order in Time Increment
Masahisa Tabata, Shoichi Fujima 177

Gas-Kinetic BGK Scheme for Hypersonic Viscous Flow
Kun Xu, Meiliang Mao 183

A Comparison of Space-Time Variational-Multiscale Discretizations
S. J. Hulshoff, E. J. Munts, R. de Borst 189

Part V Algorithms for Unsteady Flows

A Third-Order-Accurate Multidimensional Residual-Distribution Scheme for Unsteady Problems
P. De Palma, G. Pascazio, G. Rossiello, M. Napolitano 199

Unsteady Simulations for Flutter Prediction
Julien Delbove 205

Time-Accurate Navier-Stokes Calculations with Approximately Factored Implicit Schemes
Richard P. Dwight 211

Conservative Residual Distribution Schemes for General Unsteady Systems of Conservation Laws
Mario Ricchiuto, Árpád Csík, Herman Deconinck 219

Part VI Applications

Transonic Flows of BZT Fluids Through Turbine Cascades
P. Cinnella, P.M. Congedo, D. Laforgia 227

CFD Simulation of the Space Shuttle Launch Vehicle with Booster Separation Motor and Reaction Control System Plumes
L. M. Gea, D Vicker 233

An Efficient Numerical Method for 3D Viscous Ship Hydrodynamics with Free-Surface Gravity Waves
Mervyn Lewis, Barry Koren 239

Numerical Approach to the Analysis of Internal Pressure of M-V Rocket Fairing
Ayako Yamamoto, Keiichiro Fujimoto, Kozo Fujii, Nobuyuki Tsuboi 245

Automated Euler and Navier-Stokes Database Generation for a Glide-Back Booster
Neal M. Chaderjan, Stuart E. Rogers, Mike J. Aftosmis, Shishir A. Pandya, Jasim U. Ahmad, Edward Tejnil 251

Numerical Simulation of Radiative Heating for Atmospheric Reentry in Martian Atmosphere
O. Rouzaud, J. Hylkema, L. Tessé, F. Longueteau 257

An Implicit Preconditioned JFNK Method for Fully Coupled Radiating Flows. Application to Superorbital Re-Entry Simulations
R. Turpault 263

Two- and Three-Dimensional Flow Optimization in Chemical Engineering
Günter Bärwolff 271

Numerical Simulation of the Shock Wave / Boundary Layer Interaction in a Shock Tube by Using a High Resolution Monotonicity-Preserving Scheme
V. Daru, C. Tenaud 277

Accurate Flow Prediction for Store Separation from Internal Bay
M. Mani, A. Cary, W. W. Bower 283

A Coupled Navier-Stokes/Vortex-Panel Solver for the Numerical Analysis of Wind Turbines
Sven Schmitz, Jean-Jacques Chattot 289

Matematical Modeling of Supersonic Turbulent Flows in Inlets with Rotating Cowl
Bedarev I.A., Fedorova N.N., Goldfeld M.A., Falempin F. 295

Computational Fluid Dynamics of Crossflow Filtration in Suspension-Feeding Fishes
A. Y. Cheer, S. Cheung, S. L. Sanderson 301

Numerical Simulation of R-M Instability
Fu Dexun, Ma Yanwan, Tian Baolin 307

Thrust and Efficiency of Propulsion by Oscillating Foils
J. Young, J.C.S. Lai, M.Kaya, I.H. Tuncer 313

Part VII Biological Flows

Towards Numerical Simulation of Blood Flow in Small Vessels
Zinedine Khatir, Adélia Sequeira 321

Computational Fluid Dynamics and Wall Mechanics of Pre- and Post-Operative Abdominal Aortic Aneurysms
Christine M. Scotti, Ender A. Finol, Cristina H. Amon 329

Geometrical Considerations in Patient Specific Models of a Human Aorta with Stenosis and Aneurysm
Johan Svensson, Roland Gårdhagen, Matts Karlsson 335

Part VIII Flow Control

Numerical Simulation and Control of Bluff-Body Flows Using the Penalization Method
Charles-Henri Bruneau, Iraj Mortazavi, Gwendal Wilczyk 343

Application of Genetic Algorithm to Two-jet Control System On NACA 0012 Airfoil
L. Huang, R.P. LeBeau, T. Hauser 349

Reynolds-Averaged Navier-Stokes Computations of a Synthetic Jet in a Turbulent Boundary Layer
Christopher L. Rumsey 355

Active Control of Shock/Boundary Layer Interaction in Transonic Flow Over Airfoils
Jose L. Vadillo, Ramesh K. Agarwal, Ahmed A. Hassan 361

Part IX Fluid-Structure Interaction

Adaptive Solution of Some Steady-State Fluid-Structure Interactions
S. Étienne, D. Pelletier 369

Numerical Simulation for Impact of Elastic Deformable Body against Rigid Wall under Fluid Dynamic Force
Tomohisa Hashimoto, Koji Morinishi, Nobuyuki Satofuka 375

Fluid Structure Interaction of a Hypersonic Generic Body-Flap Model
Andreas Mack, Roger Schäfer, Burkard Esser, Ali Gülhan 381

The Coupled Analysis of Pipe Burst and Multicomponents Fluid of Very High Pressured Natural Gas Pipeline
Tomoe Oda, Yoshiaki Tamura, Yoichiro Matsumoto, Tetuya Kawamura 387

Part X High-Order Schemes

High-Order Residual-Based Compact Schemes
Christophe Corre, Alain Lerat 395

How Effective Are High-Order Approximations in Shock-Capturing Methods? Is There a Law of Diminishing Returns?
William J. Rider, James R. Kamm 401

Adaptive Numerical Dissipation Control in High Order Schemes for Multi-D Non-Ideal MHD
H. C. Yee, B. Sjögren. 407

A NURBS-Based Shape Optimization Method for Hydraulic Turbine Stay Vane
Didier Poueymirou-Bouchet, Christophe Tribes, Jean-Yves Trépanier . . 415

Super Compact Spatial Differencing for the Linear and Nonlinear Geophysical Fluid Dynamics Problems
V. Esfahanian, S. Ghader, A.R. Mohebalhojeh 423

A New Discretization Method of Governing Equations for High Order Accuracy
Dehee Kim, Jang Hyuk Kwon 429

A High-Order Accurate Unstructured GMRES Solver for the Compressible Euler Equations
Amir Nejat, Carl Ollivier-Gooch 435

Computation of Aeroacoustic Waves with High Order Spectral Volume Method
Z.J. Wang 441

Discontinuous Spectral Difference Method for Conservation Laws on Unstructured Grids
Yen Liu, Marcel Vinokur, Z.J. Wang 449

Multigrid Solution for High-Order Discontinuous Galerkin Discretizations of the Compressible Navier-Stokes Equations
Todd A. Oliver, Krzysztof J. Fidkowski, David L. Darmofal 455

Part XI Incompressible Flow

Accurate Solution of Corner Singularities in Axisymmetric and Plane Flows Using Adjusted Mesh of Finite Elements
Pavel Burda, Jaroslav Novotný, Jakub Šístek 463

Sensitivity Analysis of Transient Incompressible Laminar Flows
H. Hristova, S. Etienne, D. Pelletier, J. Borggaard 469

Comparison of Artificial Compressibility Methods
Cetin Kiris, Jeffrey Housman, Dochan Kwak 475

Part XII Magnetohydrodynamics

A Central, Diamond-Staggered Dual Cell, Finite Volume Method for Ideal Magnetohydrodynamics
P. Arminjon, R. Touma 483

Simulation of Supersonic Flows in Inductively Coupled Plasma Tunnels
James R. Diebel, Thierry E. Magin, Marco Panesi, Pietro Rini, David Vanden Abeele, Gérard Degrez 489

Drift-Diffusion Model for Magneto-Fluid-Dynamics Interaction
J.S. Shang, S.T. Surzhikov 495

Part XIII Meshless Methods

Gridless Computation Using the Unified Coordinates
W.H. Hui, J.J. Hu, G.P. Zhao 503

Viscous Flow Computations Using a Meshless Solver, LSFU-U
Anup Ninawe, N. Munikrishna, N. Balakrishnan 509

Part XIV Microscale Flows

Preconditioning Method for Compressible Near-critical Fluids in Micro-Channel
Satoru Yamamoto 517

Comparison of Kinetic and Navier-Stokes Solutions for Rarefied Gas Flows in Micro-channels
Nobuyuki Satofuka, Koji Morinishi, Keigo Kamitsuji 523

Application of the 10-Moment Model to MEMS Flows
Yoshifumi Suzuki, Shintaro Yamamoto, Bram van Leer, Quanhua Sun, Iain D. Boyd 529

Part XV Modelling and Simulation of Turbulence

Calculation of Static and Dynamic Stability Derivatives of the F/A-18E in Abrupt Wing Stall Using RANS and DES
James R. Forsythe, Charles M. Fremaux, Robert M. Hall..... 537

Large Eddy Simulation of Flow Around a Slat with a Blunt Trailing Edge
Saloua Ben Khelil..... 543

Implicit Large Eddy Simulation of a Flow Around a Subsonic Airfoil Near its Stall Angle
Satoko Komurasaki, Kunio Kuwahara 549

DNS of Compressible Turbulent Boundary Layer Over a Blunt Wedge
Xinliang Li, Derun Fu..... 555

Computation of the Turbulent Boundary Layer on a Long Circular Cylinder in Axial Flow with a Vorticity Boundary Condition
Milton Woods, Max Bull 561

LES of Combined Forced and Natural Turbulent Convection in a Vertical Slot
J. Yin, D.J. Bergstrom 567

Numerical Study on $k - \omega$ Turbulence Models for Supersonic Impinging Jet Flow Field
Eugene Kim, Soo Hyung Park, Jang Hyuk Kwon..... 573

Comparative Study of Reynolds Stress Turbulence Models in Free-Shear and Wall-Bounded Flows
Valerio Viti, George Huang, Peter Bradshaw 579

Part XVI Multifluid and Multiphase Flows

Lattice Boltzmann Simulations in Chemical Engineering
D. Hänel, U. Lantermann, R. Kaiser 587

A Numerical Scheme for Compressible Multiphase Flows
Rémi Abgrall and Vincent Perrier..... 593

A New Accurate Method for Simulating Polydispersed Two-Phase Flows
G. Dufour 601

The Characteristics-Based Matching Method (CBM) for High-Speed Fluid-Fluid Flows
Nourgaliev, R.R., Dinh, T.N., Liou, M.-S., Theofanous T.G. 607

Simulation of Multifluid Multiphase Flows with AUSM⁺-up Scheme
Chih-Hao Chang, Meng-Sing Liou..... 613

Computational Framework for Complex Fluid Physics Applications
Ding Li, Guoping Xia, Venkateswaran Sankaran, Charles L. Merkle ... 619

A Novel Physical Model and Computational Method for Non-Isentropic, Compressible Two-Fluid Flow
Jeroen Wackers, Barry Koren 625

Modeling Turbulent Interfacial Flows
Ali Jafari, Nasser Ashgriz..... 631

On Modeling of Collisions in Direct Numerical Simulation of High-Speed Multiphase Flows
Nourgaliev, R.R., Dinh, T.N., Theofanous T.G...... 637

A Second-Order Adaptive Sharp-Interface Method for Incompressible Multiphase Flow
M. Sussman, M.Y. Hussaini, K. M. Smith, Ren Zhi-Wei, V. Mihalef .. 643

Large-Scale Direct Simulation of Two-Phase Flow Structure Around a Spacer in a Tight-Lattice Nuclear Fuel Bundle
Kazuyuki Takase, Hiroyuki Yoshida, Yasuo Ose, Hajime Akimoto 649

Part XVII Optimization

Surface Mesh Movement for Aerodynamic Design of Body-Installation Junction
Hyoung-Jin Kim, Kazuhiro Nakahashi 657

Formulation and Multigrid Solution of the Discrete Adjoint Problem on Unstructured Meshes
Dimitri J. Mavriplis 663

Aerodynamic Design of Gas Turbine Cascades Using Global Optimizers and Artificial Neural Networks
Temesgen Mengistu, Wahid Ghaly..... 669

An Analysis of Bodies Having Minimum Pressure Drag in Supersonic Flow: Exploring the Nonlinear Domain
Karthik Palaniappan, Antony Jameson 675

Optimum Multidisciplinary and Multi-Objective Wing Design in CFD Using Evolutionary Techniques
L. González, E. Whitney, K. Srinivas, J. Périaux 681

Advances in Aerodynamic Shape Optimization
Antony Jameson 687

On the Use of Parametric-CAD Systems and Cartesian Methods for Aerodynamic Design
Marian Nemec, Michael J. Aftosmis, Thomas H. Pulliam 699

Improvement of the Optimization Method of the TSTO Configuration – Application of Accurate Aerodynamics
Koji Shimoyama, Kozo Fujii, Hiroaki Kobayashi 705

Part XVIII Parallel Algorithms

Parallel Simulation for Strong Blast Wave from TNT Explosion on Large-scale PC-Cluster
Takayuki Aoki, Kaori Kato, Tei Saburi, Masatake Yoshida 713

A Parallel Implicit Adaptive Mesh Refinement Algorithm for Body-Fitted Multi-Block Mesh
Clinton P. T. Groth..... 719

MPI Parallelization of Unstructured Mesh Adaptation
C.Y. Lepage, A. St-Cyr, W.G. Habashi..... 727

Parallel Implementation of a Dynamic Overset Unstructured Grid Approach	
<i>A. Madrane</i>	733
A Parallel Multi-Block Method for the Unsteady Vorticity-Velocity Navier-Stokes Equations	
<i>A. Grimaldi, G. Pascazio, M. Napolitano</i>	741
Parallelization of an Unstructured Data Based Cell Centre Finite Volume Code, HIFUN-3D	
<i>Gopal N. Shinde, Nikhil V. Shende, N. Balakrishnan</i>	747
Parallel Turbulent Flow Computations Using a Hybrid Spectral/Finite-Element Method on Beowulf Clusters	
<i>David Vanden-Abeelee, Gérard Degrez, Deryl Owen Snyder</i>	753
<hr/>	
Part XIX Upwind Schemes	
<hr/>	
An Upwind Moment Scheme for Conservation Laws	
<i>H. T. Huynh</i>	761
Accurate and Efficient Re-evaluation of Cell-interface Convective Fluxes	
<i>Sung-Hwan Yoon, Kyu-Hong Kim, Chongam Kim, Oh-Hyun Rho</i>	767
Computation of The Flow Around a Bluff Body By Multi-Directional Finite Difference Method	
<i>Mi Young Lee, Tetuya Kawamura, Kunio Kuwahara</i>	773
A One Point Shock Capturing Kinetic Scheme for Hyperbolic Conservation Laws	
<i>Dominic D.J. Chandar, S.V. Raghurama Rao, S.M. Deshpande</i>	779
Accurate and Efficient Multi-dimensional TVD Interpolation	
<i>Sung-soo Kim, Kyu-Hong Kim, Chongam Kim</i>	785
Exact Flux Linearization for Convergence Improvement in the Implicit Godunov Method	
<i>Igor Men'shov, Yoshiaki Nakamura</i>	791
On High-Order Fluctuation-Splitting Schemes for Navier-Stokes Equations	
<i>Hiroaki Nishikawa, Philip Roe</i>	799
Computation of Weakly Ionized Atmospheric Entry Flows Using an Extended Roe Scheme	
<i>Tristan Soubri�e, Olivier Rouzaud, Jouke Hylkema</i>	805

Part XX Technical Notes

3D Prediction of Developing Turbulent Flow in a 90° Duct of Rectangular Cross-Section
H. Alemi, M. Raisee 813

Numerical Simulation of Steady Newtonian and Non-Newtonian Flow Through Vascular Stenoses
Geoffrey R. Behrens, Ramesh K. Agarwal 815

Finite Volume Methods for Fluid Flow Through Elastic Tubes
Marek Brandner 817

Parallel 2D/3D Unsteady Incompressible Viscous Flow Computations Using an Unstructured CFD Code
H. Chen, P.G. Huang, R.P. LeBeau 819

Adaptive Bounds to Outputs of the Three Dimensional Steady Incompressible Navier-Stokes Equations
Hae-Won Choi, Marius Paraschivoiu 821

A Comparative Study of Three Composite Schemes: Lax-Wendroff/Lax-Friedrichs, Mac-Cormack/Lax-Friedrichs and Corrected Lax-Friedrichs Lax-FriedrichS Schemes, Based on Conservation Laws
M.Z. Dauhoo, A.R. Appadu 823

Evaluation of Reynolds Number Effects on the CFD Simulation of Downwind Sails
G. Delussu, N. Erriu, R.G.J. Flay, M. Mulas, P. Puddu, M. Talice ... 825

Assessment of the Immersed Boundary Technique for Compressible CFD codes
G. Delussu, M.Mulas, M. Talice 827

Spectral Solution of High Speed Flows Over Blunt Bodies with Improved Boundary Treatment
V. Esfahanian, M. Boroomand, M. Najafi 829

Verification of Mathematical Model of the Shock Wave/Dust Layer Interaction Problem
A.V. Fedorov, N.N. Fedorova, I.A. Fedorchenko 831

Automated Unstructured Mesh Generation for Objects in Direct Contact
Dr. F. Fortin, T. Zoric 833

Complex Flow Patterns in Realistic Geometry of Human Aorta <i>R. Gårdhagen, J. Svensson, M. Karlsson</i>	835
Interplay Between Inertia and Gravity in Transient Thin-Jet Flow <i>Radoslav German, Roger E. Khayat</i>	837
Numerical Modeling of Cell Deformation Passing Through a Nozzle to Determine its Viscosity and Surface Tension <i>Amirreza Golpaygan, Nasser Ashgriz</i>	839
Gradient Computation for Variational Assimilation of Meteorological Observations <i>Y. Horibata</i>	841
3-D Heat and Fluid Flow Analysis of Successively Variable Louver Angle of Louver Fin Geometry in Compact Heat Exchangers <i>C. T. Hsieh, J. Y. Jang</i>	843
Pattern Formation in Viscoelastic Thermal Convection <i>Zhenyu Li, Roger Khayat</i>	845
Turbulent Transport of Passive Scalar Emitted from Line Sources in an Open Channel Flow <i>Chun-Ho Liu, Dennis Y.C. Leung</i>	847
Mass Transpiration Cooling Analysis at Hypersonic Mach Numbers Using CFD Tools <i>P.S. Kulkarni, V.N. Kulkarni, K.P.J. Reddy, T. Saito, K. Takayama</i> . .	849
FEM in Domain Decomposition for Fluid-Structure Interaction Problems <i>Pavel Moses, Jaroslav Novotný, Pavel Burda</i>	851
LES of Turbulent Flow Around a Simplified Railway Vehicle Model Under Cross Winds <i>Koji Nakade, Masahiro Suzuki</i>	853
Development of Compressible Navier-Stokes Equations into Higher Order DNS of Incompressible Turbulence <i>Hidetoshi Nishida, Motoyoshi Hatta</i>	855
Direct Numerical Simulation of Mixed Convection in Horizontal Pipe Flow <i>M. Piller</i>	857

Simulation of Inviscid, Unsteady Flows in Hypersonic Air Inlets Using an Adaptive, Unstructured, Multi-Block Method
Râbi Bin Tahir, Eugene Timofeev, Peter Voinovich, Sannu Mölder 859

Fluid Structure Interaction for Strongly Coupled Problems Based on a Sensitivity Analysis
Jan Vierendeels, Kris Dumont, Erik Dick, Pascal Verdonck 861

Numerical Simulation of Flow Conditioners Used for Flow Meter Calibration
E. von Lavante, G. Moniz Pereira, U. Banaszak, B. Mickan 863

Large Eddy Simulation Using Tetrahedral Elements
Tao Xu, German Cardenas, Marius Paraschivoiu 865

Part I

Invited Lectures

Topics in Detached-Eddy Simulation

Philippe R. Spalart

Boeing Commercial Airplanes, P.O. Box 3707, Seattle, WA 98124, USA
philippe.r.spalart@boeing.com

The paper re-visits the motivation of DES, and then touches on its diffusion in CFD codes; grid concerns including both users' mis-conceptions and actual DES issues; the use of DES as a pure LES with wall modeling; and possible long-term improvements.

1 Introduction

The DES approach to high-Reynolds-number separated flows is seven years old [1], although the first true results appeared only five years ago [2]. Its best description is in [3], and a broader review in [4]. The central motivation is the observation that Large-Eddy Simulation (LES) is powerful in regions of massive separation and other free shear flows such as jets, but much too costly in the large areas of thin boundary layers (BL's) which cover aircraft and vehicles. Therefore, affordable CFD approaches need to treat these with Reynolds-Averaged modeling. No theoretical rebuttal has been made by LES proponents of this pessimistic statement, which has had an influence at least in Europe. Even as a "grand challenge" and with generous assumptions, the estimated readiness date of pure LES for a wing remains at the year 2045.

On the other hand, progress in Reynolds-Averaged Navier-Stokes (RANS) models outside thin shear flows has remained very modest, whether in terms of the numerical practicality of the models, or their accuracy. The two dominant models are 12 years old. This field being idea-limited, a "readiness date" cannot be projected. The pessimistic view is that a general RANS model with certain engineering accuracy is out of reach of human intelligence. However, keeping the other sources of error in CFD below engineering accuracy will never be certain either, considering the users' training and their need for rapid answers. In any case, RANS has its place, especially for attached flows which place low demands both on the models' physics and the users' competence.

The LES cost estimates of 1997 [1] can be confronted with recent findings. Even forceful studies such as LESFOIL found that in 2002 the limit on the spanwise domain size for LES of an airfoil was near 1% of its chord [5, 6] which is insufficient when the BL thickness δ exceeds 8%. Over the trailing edge, even the best Reynolds stresses were not very close to experiment. Now, extrapolating to the wing considered in [1, 4], its turbulent domain is 2,000

times larger, and the time interval much longer. Since the ONERA LES used 6 million points per side of the airfoil and per % of chord, without a turbulent leading edge or lower surface, the extrapolation to a wing leads to well over 10^{10} points, which is consistent with the estimate of 10^{11} in [4]. Recall that it is a weak function of Reynolds number (because under the assumptions made for wall modeling, only the slow thinning of the BL influences the cost).

The very resilient issues with LES and RANS led to a consensus in many circles that RANS/LES hybrid methods are the only ones with a chance in external separated flows, and to the creation of other hybrids, in particular LNS and SAS [7, 8].

These other, more recent hybrids have not yet spread outside the groups that created them but DES has, and is offered in vendor CFD codes including Cobalt, CFD++, STAR-CD, Acusolve and Fluent [9, 10]. Their capability to resolve “LES content”, with short waves and high frequencies, needs to be verified; Cobalt results have been impressive. It is not clear what proportion of users can make an accurate use of DES, because significant additional decisions must be made for the grid and time step, relative to RANS CFD, and a substantial increase in cost must be accepted. It appears that the vendors provide publications and consultation to new DES users, rather than comprehensive sets of instructions. A manual for DES grid design is found at <http://techreports.larc.nasa.gov/ltrs/PDF/2001/cr/NASA-2001-cr211032.pdf>. However, no manual can be a substitute for the combination of experience, intuition for separation and turbulence, and effort in visualizing solutions. Also essential is a willingness to apply grid refinement, and to admit that CFD is not yet able to produce an accurate solution when the problem is simply too challenging. Examples would be: an aircraft with Active Flow Control through a tiny suction slot; a complete car; and a prediction of noise over the entire audible range. Yet, these tasks are in high demand.

2 Grid Issues

2.1 Expectations for grid count

In some studies, DES is compared with LES on the same flow, and is expected to provide similar accuracy on a *coarser* grid than LES. This is most often incorrect. If a pure LES is possible, the flow cannot contain extended turbulent BL's. The BL's, probably, are simply laminar, so that DES does not provide its fundamental additional capability over LES. The difficulty resides in the region of massive separation, and there is no reason why DES would accept a coarser grid than LES does. The DES SGS model is one among many plausible ones. Therefore, it is fair to compare DES and LES on the same grid, and to count that DES can also treat the flow at high Reynolds numbers with turbulent BL's, *without* a dramatic reduction of the grid spacing [3].

Another error is apparent in some LES studies of flows with turbulent BL's. These used pure SGS models such as Smagorinsky's or its dynamic derivative in those BL's, with grids much too coarse to resolve the BL eddies. Such simulations are, effectively, DES with an inappropriate RANS model, one which has no credentials to simulate an entire BL. The eddy viscosity is, furthermore, grid-dependent even in the attached BL, which would result in a continued drift of the separation point if the grid were refined.

Grid refinement in unsteady three-dimensional simulations is very demanding. A refinement that doubles the total number of points is questionable. An unquestionable refinement consists in doubling the number of points in every direction, and the number of time steps. This raises the cost by a factor of 16, and is rarely achieved. A fair compromise is to use a factor of $\sqrt{2}$ in each direction, especially if this is done twice [3]. With second-order numerics and a given equation, such a refinement reduces the error by half. The situation in DES and LES is not as simple, because the differential equation depends on the grid spacing, and the order of accuracy depends on which quantity is considered. Nevertheless, if an LES were grossly under-resolved, it is very unlikely that a refinement by $\sqrt{2}$ would fail to reveal it.

Refining the grid in only one or two directions is not consistent, unless the coarse run has given strong evidence that only these directions were under-resolved. In [11], the spanwise grid spacing Δz around a cylinder was left the same while the x - y grid was refined. Furthermore, Δz was already larger than the x - y spacings in the sensitive region, so that the capability to resolve eddies was unchanged. The refinement was illusory. In contrast, Morton *et al.* applied systematic refinement via a parameter in the grid generation [10].

The common approach is to learn about the flow from simulations on relatively coarse grids and to generate grids that are finer by the factor $\sqrt{2}$ in the more sensitive regions, but not everywhere [3]. The grid is optimized, based on flow visualizations. The grid count does not quite rise by $\sqrt{8}$ but, in the user's judgment, the quality of the resolution did improve by $\sqrt{2}$. The neatest package would come from re-running the coarse simulation on a grid obtained by uniformly de-refining the optimized fine grid.

2.2 Grey Area, Ambiguous Grids and "Grid-Induced Separation"

Concurrently with its encouraging results on airfoils, thin wings, and cylinders, weaknesses of DES were discovered, notably by Caruelle, Deck, and Menter [12, 13]. It was always recognized that the location of separation will always be controlled by the RANS model, so that perfection is not expected, no matter how fine the grid. The primary new concern is that, starting from a valid RANS solution (Type I in fig.1), gradually refining the grid alters the solution in obscure ways. In the extreme, it leads to a serious problem, called "Grid-Induced Separation" (GIS) by Menter [13]. It was not anticipated in [1] that simulations would encounter this with grids intended for the RANS mode, but the evidence is here. The reduced grid spacing begins

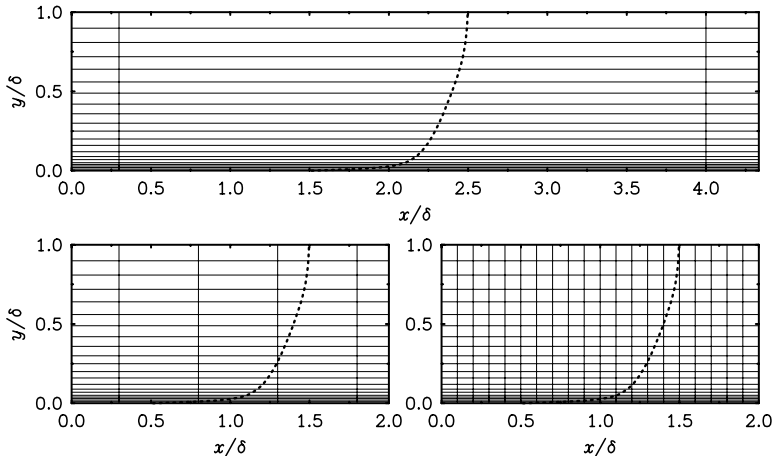


Fig. 1. DES grids in a boundary layer. Top, Type I, natural DES; left, Type II, ambiguous spacing; right, Type III, LES. See section 2.2 and 3. ---, mean velocity. δ is BL thickness. Assume $\Delta z \approx \Delta x$.

to lower the eddy viscosity, in the direction of LES, but not enough to allow “LES content” (eddies) to develop. The grid is “ambiguous” (Type II) and the DES equations fail to recognize that pure RANS behavior was intended. The solution then is essentially a RANS with too weak an eddy viscosity; the strongest symptom is premature separation. Furthermore, DES fails to give much of a signal of this failure. Sometimes, GIS results from refining the grid to a spacing that is un-necessarily fine, and regions in which the wall-parallel spacing is very fine in both directions cannot be extensive, simply because the grid count would be extremely large. For instance, an efficient grid adaptation at the foot of a shock wave would refine the spacing only normal to the shock, and therefore not cause GIS. In that sense, two-dimensional exercises as in [13] over-state the GIS issue. DES, of course, is never two-dimensional. Nevertheless, the ideal hybrid method would never produce GIS, even with substantial thickening of the BL. Some effort was applied against GIS but without much success, at least if the modifications are required to preserve the simplicity of the DES equations and avoid zonal divisions.

A related danger is that such an un-intended drop of eddy viscosity can fortuitously improve these near-RANS predictions, because turbulence models fail somewhat more often by producing an excess than a deficit of eddy viscosity. See, for instance, the difference between Menter’s BSL and SST models: SST is the favorite, and always returns a lower eddy viscosity and therefore earlier separation. Also observe that all simple models produce far too much eddy viscosity inside vortices. It is much preferable not to attribute to DES an improvement which is not deserved, and would overshoot if the grid were refined further (but still short of LES mode).

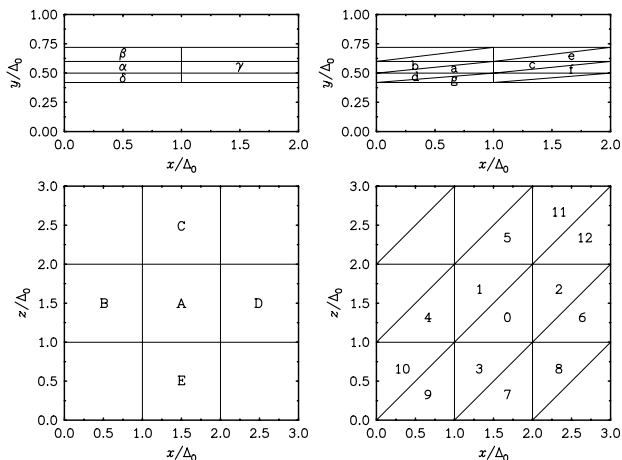


Fig. 2. Possible grid arrangements in a BL. Upper frames, side views; lower frames, top views. Left frames, structured grids; right frames, regular prisms or tetrahedra.

2.3 Definition of Δ in unstructured grids

The length scale Δ controls the eddy viscosity in the LES regions. The definition of DES [1] included $\Delta \equiv \max(\Delta x, \Delta y, \Delta z)$, for structured grids. A clear statement for unstructured grids is essential now that such codes are running DES. Figure 2 illustrates the challenge in a BL. The cell names are placed at the cell centroids. The target for Δ is Δ_0 , at least at first sight. This is natural in the structured hexahedral grids on the left, where the distances taken will be from α to γ and from A to B, for instance. On the right, the grids are regular, but considered as unstructured. A common grid type is with prisms, which look like the upper-left frame from the side, and the lower-right frame from the top. Considering cell 0, the natural procedure will be to calculate the distance only to 1-3, the cells which share a face with 0. Then, Δ will be only $\Delta_0\sqrt{5}/3$, or about $0.75\Delta_0$. If cells that share only a corner are included, cells 4-7 give Δ_0 , but cells 10-11 drive Δ to $\Delta_0\sqrt{20}/3$, which is much larger. The cell diameter is $\sqrt{2}\Delta_0$ (or a little more, because of the cell thickness in 3D). For consistency with the cubic cells of the 3D simulations used to set the value of C_{DES} , the diameter would be divided by $\sqrt{3}$. Therefore, the diameter measure finally gives $\sqrt{2/3}\Delta_0$, which appears satisfactory.

A more subtle question is: what is the legitimate value for Δ in this prism grid? It has twice the degrees of freedom of the hexahedral grid, but is the effective resolution better by $\sqrt{2}$? The diameter of the cells is a plausible measure, since it is the longest distance over which some derivative of the function is assumed to be uniform in the re-construction scheme. The diameter of the triangles is the same as that of the squares. On the other hand, the average distance to the points (1-3) used to calculate the gradient is also a

plausible measure, and is not far from $\Delta_0/\sqrt{2}$. In the end, the effect is weak for prisms, and C_{DES} has never been a sensitive constant.

The effect could be stronger for other cell shapes, such as tetrahedra, and arrangements. These will not be analyzed here, but code writers should be aware. In no situation should the scale Δ reduce to a distance similar to that from a to g in the upper-right frame. In general, using for Δ the cell diameter, divided by $\sqrt{3}$, appears to be the safest approach.

3 Use of DES as a pure LES

3.1 Analysis of the channel-flow DES study by Nikitin *et al.*

The paper, NNWSS in short, addressed the simplest of candidates for LES among wall-bounded flows [14]. The objective was to understand the behavior of DES in a thick BL with a grid fine enough for LES mode inside it (Type III). This is an “un-natural” use of DES, but some geometries will impose it, and it also is the only possible solution to the issue that no RANS model will ever give a perfect prediction of separation and reattachment. This type of DES can also be viewed as an LES with “wall modeling”. This makes it a candidate for atmospheric BL simulations, for instance; it has unlimited Reynolds-number capability, and the S-A model can treat rough surfaces.

In the NNWSS work, DES functioned as expected, as an unsteady RANS very near the wall and an LES in the center of the channel. This has not been achieved by other RANS-LES hybrids, nor by SAS [8]. The velocity profiles revealed the expected “modeled log layer” very near the wall, and “resolved log layer” part-way up the BL. These two layers matched in slope (the Kármán constant κ), but not in level (the intercept C). Some observers took this as a substantial failure of DES, thus failing to appreciate several crucial aspects of that work.

The study was conducted under very tight constraints. The formulas of DES were used without any adjustments for this new rôle, and fit in a small space; simplicity and clarity are tangible advantages for any model, as confirmed by the agreement between three different codes. The grids had identical spacings in the wall-parallel directions, therefore indifferent to the flow direction; the spacing strategy in the wall-normal direction was systematic. A Reynolds number Re_τ of 80,000, far out of reach of DNS, was reached on modest computers. Substantial grid refinement was conducted, and simply lowered the RANS/LES interface without disturbing either of the log layers.

This should be compared with the countless channel “LES” studies which hardly exceed the Reynolds numbers accessible to DNS, even with massive computing resources, or to the studies that involve highly complex sub-grid-scale (SGS) and wall models, or two zones. These would be difficult to extend to general geometries; often, they are not even clearly defined in the publication. They contain numerous disposable constants. The height of this

practice is when the Kármán “constant” used in the model is subjected to large variations. Not only is this against any theory, but it would destroy the accuracy at high Reynolds numbers. In most of the studies NNWSS can be compared with, grids are finer in the spanwise direction than in the flow direction, which is practical only in the simplest of flows. Some SGS models have stability problems, and require averaging in the wall-parallel or other homogeneous directions; this is inconsistent with the idea that a dynamic model responds to local conditions better than an algebraic model such as Smagorinsky’s. It also makes them far from ready for non-trivial geometries. NNWSS had no such issues. DES provides a dynamic SGS model, in a sense, but makes no claims that it has better physics than an algebraic model; simply, it is done to unify the LES treatment with the RANS treatment.

A full and simple solution to the log-layer mismatch in DES has not been found, and flow visualizations examined after the paper went to press were disappointing in that the near-wall structures were much weaker and more elongated than expected [15]. An expedient solution is to re-set the resolved log layer by offsetting the modeled log layer; this is achieved by changing the c_{v1} constant of the S-A model from 7.1 to 4 [14], and restores the skin-friction coefficient C_f to a correct level, from a level that is about 15% too low. Piomelli *et al.* addressed the deeper problem by intensifying the resolved turbulence with random forcing, applying a “backscatter model” [15]. Unfortunately, this requires explicit intervention and extra parameters, which is a serious obstacle to routine use. The method loses its readiness for general geometries and grids, and the user burden is higher.

3.2 Switch from RANS to LES mode within an attached boundary layer

RANS is best where the BL is thinnest while, at least in a research exercise such as LESFOIL, LES could be the final answer to separation prediction. This is because it would reduce the rôle of empiricism, increasingly as the grid is refined. DES allows LES to be initiated after the BL has transitioned and thickened sufficiently, but well before separation. This would make a “DESFOIL” very competitive, although delicate; it must not allow any ambiguous-grid situation, and LES content must be created deliberately. An abrupt change in grid spacing near 35% chord, from Type I to Type III, will prevent GIS, and the challenge is to generate mature LES content within as short a space as possible. There is a single solution field, only with special measures locally to “trip” the BL. It is known that raw random numbers do not meet this challenge: the “turbulence” takes many BL thicknesses to recover. A very useful alternative is the recycling method of Lund *et al* [16]. It has been very effective for BL’s without pressure gradient, and can be greatly simplified; its extension to pressure gradients appears manageable in 2D.

4 Long-term improvements

4.1 Optimization of the RANS model

The remaining rôle of the model is in BL's, and shallow separation bubbles. This motivated the introduction of the SST model in DES [17], but there would be no sense in going beyond two equations. The essence of DES is to employ simple RANS models, tuned for thin shear layers. It would be logical to re-calibrate the model for these flows only, ignoring the free shear flows which normally are in LES mode. This would give the same number of adjustable parameters for a smaller class of flows. The obstacle is that achieving a level of accuracy that is conclusively superior will require excellent accuracy in experiment and calculations for a large number of flows. Recent findings on wind-tunnel wall effects, for instance, are poor omens of this [18]. Also note how the value of the Kármán constant has been challenged by recent experiments, so that the accepted range of $[0.40, 0.41]$ has given way to $[0.38, 0.436]$, which is wide. This is the most fundamental of constants in a BL model, so that perfection for a RANS model, even in BL's only, is as elusive as ever.

4.2 Solution to ambiguous grids

A proposal derives from the observation that GIS occurs in RANS-type grids that still have BL character, that is, shallow cells (figure 1). The DES length-scale limiter starts controlling \tilde{d} when Δ is less than $d/0.65$, whereas the wall-normal spacing Δn is usually less than $d/10$. Therefore, there is a range of situations for which the cell aspect ratio AR could be a tool. Δ would be multiplied by a function of AR that equals 1 for AR near 1, so that it is passive in normal LES grids, and exceeds 1 for higher values of AR. There are concerns over regions away from the wall where the grid may have high aspect ratio, either fortuitously or because of adaptation to a thin flow feature. It was tested with only moderate success by J. Forsythe (personal communication, 2003), who will at this meeting present an alternate proposal, based on a function of d and $C_{DES}\Delta$ that is not simply their minimum, but instead overshoots $C_{DES}\Delta$ when they are nearly equal. This must be viewed as a partial solution, just like the use of AR, because it contains a parameter that limits by how much \tilde{d} can exceed $C_{DES}\Delta$. Therefore, further refinement will defeat them, unless the user explores the solution and raises the limit again, which is somewhat against the spirit of DES.

Menter *et al.* use the F_2 function to disable the limiter inside a BL, for the SST version of DES [13]. Only sudden separation can drive the length scale $2k^{3/2}/\epsilon$ small enough, relative to the wall distance d , for LES mode to begin. This approach favors the RANS mode of DES. It seems to increase the possibilities for multiple solutions. A version for S-A with $F_2(r)$ will be tested.

4.3 Other challenges

Automatic grid adaptation is a major goal for industrial CFD codes. Adaptation in steady solutions is taking a more mathematical turn, with adjoint methods in particular, and emphasizes anisotropic refinement to shear layers and shock waves. Adaptation in DES has started, but is isotropic away from walls and remains more empirical, typically being based on mean vorticity [19].

Another legitimate need of engineering practice is error estimation. The drag of an airliner does not need to be known “as closely as possible”; it needs to be known to better than 1%. Scientific journals also ask for the numerical uncertainty to be “accurately quantified”, and a true answer is usually impossible. This is already very difficult for the numerical errors, more difficult for the LES errors, and near-impossible for the RANS errors. Numerical errors may eventually be estimated from a single solution. LES errors can be scoped by vigorous grid refinement. RANS errors can be scoped by switching models, but not reliably. It is possible for a new flow type to make all the models err in the same direction, so that a test between models is not instructive. The free vortex seems to be a clear example of that. In all cases, real-life geometries with a very different level of sensitivity in different regions pose much more difficult problems than simple geometries.

5 Summary

DES has been rather successful and well-understood, and has not required any essential modification since its creation in 1997. However, perfection is not expected from any method in an endeavor as complex as the numerical prediction of turbulence, especially since the numerical power at the engineers’ disposal remains marginal for many “real-life” problems, and utterly insufficient for the rest. Therefore, RANS-LES hybrids will be helpful for many years, but user training and judgment will be essential as will experience sharing via publications. Not only is the approach imperfect, but it can be mis-used; in that sense, robustness almost becomes a liability. Fully solving the issue of ambiguous grids is a priority, but has proven to be a resilient difficulty. The RANS component also may be improved, with the usual emphasis on separation. Another welcome change would be a numerically efficient system to control laminar regions; a magnificent one would be to predict transition, within the Navier-Stokes solution and even in unstructured grids.

Acknowledgements

The author is highly grateful for the extensive simulations and numerous fruitful discussions he owes to Prof. M. Strelets and his group, to Prof. K. Squires, and to Dr. J. Forsythe.

References

1. P. R. Spalart, W.-H. Jou, M. Strelets, S. R. Allmaras: Comments on the feasibility of LES for wings, and on a hybrid RANS/LES approach. First AFOSR International Conference on DNS/LES, Aug. 4-8 1997, Ruston, Louisiana.
2. M. Shur, P. R. Spalart, M. Strelets, A. Travin: Detached-eddy simulation of an airfoil at high angle of attack. 4th Int. Symp. Eng. Turb. Modelling and Measurements, May 24-26 1999, Corsica. Elsevier.
3. A. Travin, M. Shur, M. Strelets, P. Spalart: Detached- Eddy Simulations past a Circular Cylinder. *Flow, Turb. Comb.* **63**, 293 (2000).
4. P. Spalart: Strategies for turbulence modelling and simulations. *Int. J. Heat Fluid Flow.* **21**, 252 (2000).
5. C. P. Mellen, J. Fröhlich, W. Rodi: Lessons from the European LESFOIL project on LES of flow around an airfoil. *AIAA J.* **41**, 4:573-581 (2003).
6. I. Mary, P. Sagaut: Large eddy simulation of flow around an airfoil near stall. *AIAA J.* **40**, 6:1139-1145 (2002).
7. P. Batten, U. Goldberg, S. Chakravarthy: LNS – an approach towards embedded LES. AIAA-2002-0427.
8. F. R. Menter, M. Kuntz, R. Bender: A scale-adaptive simulation model for turbulent flow predictions. AIAA 2003-0767.
9. R. Allen, F. Mendonça, D. Kirkham: RANS and DES turbulence model predictions of noise on the M219 cavity at $M=0.85$. Colloquium EUROMECH 449, Dec. 9-12 2003, Chamonix, France.
10. S. A. Morton, J. R. Forsythe, K. D. Squires, K. E. Wurtzler: Assessment of unstructured grids for detached-eddy simulation of high Reynolds number separated flows. 8th ISGG Conf., Honolulu, June 2002.
11. M. Breuer, N. Jovičić, K. Mazaev: Comparison of DES, RANS and LES for the separated flow around a flat plate at high incidence. *Int. J. Num. Meth. in Fluids.* **41**:357-388 (2003).
12. S. Deck, E. Garnier, P. Guillen: Turbulence modelling applied to space launcher configurations. *J. Turbulence* **3** (2002).
13. F. R. Menter, M. Kuntz, L. Durand: Adaptation of eddy viscosity turbulence models to unsteady separated flow behind vehicles. Symp. “The aerodynamics of heavy vehicles: trucks, buses and trains”. Monterey, USA, Dec. 2-6 2002.
14. N. V. Nikitin, F. Nicoud, B. Wasistho, K. D. Squires, P. R. Spalart: An Approach to Wall Modeling in Large-Eddy Simulations. *Phys. Fluids* **12**, 7 (2000).
15. U. Piomelli, E. Balaras, H. Pasinato, K. D. Squires, P. R. Spalart: The inner-outer layer interface in large-eddy simulations with wall-layer models. *Int. J. Heat Fluid Flow* **24**:538-550 (2003).
16. T. S. Lund, X. Wu, K. D. Squires: Generation of turbulent inflow data for spatially-developing boundary layer simulations. *J. Comp. Phys.* **140**:233-258 (1998).
17. M. Strelets: Detached Eddy Simulation of massively separated flows. AIAA-2001-0879.
18. A. Garbaruk, M. Shur, M. Strelets, P. R. Spalart: Numerical study of wind-tunnel wall effects on transonic airfoil flows. *AIAA J.* **41** 6:1046-1054 (2003).
19. S. A. Morton, M. B. Steenman, R. M. Cummings, J. R. Forsythe: DES grid resolution issues for vortical flows on a delta wing and an F-18C. AIAA-2003-1103.

High-End Computing Challenges in Aerospace Design and Engineering

F. Ronald Bailey

Advanced Management Technology Inc., M.S. 258-6, NASA Ames Research Center, Moffett Field, CA 94035-1000. fbailey@mail.arc.nasa.gov

Abstract

High-End Computing (HEC) has had significant impact on aerospace design and engineering and is poised to make even more in the future. In this paper we describe four aerospace design and engineering challenges: Digital Flight, Launch Simulation, Liquid Rocket Engine Fuel System and Digital Astronaut. The paper discusses modeling capabilities needed for each challenge and presents projections of future near and far-term HEC computing requirements. NASA's HEC Project Columbia is described and programming strategies presented that are necessary to achieve high real performance

1 Introduction

High-End Computing (HEC) has had a major impact on design and engineering in the aerospace industry. HEC simulation is routinely used to improve understanding of complex physics phenomenon and thus lead to improved design solutions. HEC is enabling the use of CFD to significantly reduce wind-tunnel testing in vehicle design and to provide data that cannot be obtained by wind-tunnel experiments. None of these would be possible without the more than five orders-of-magnitude increase in HEC performance over the past three decades, which, in turn, has motivated the development of models of increasing fidelity and complexity. As a result, HEC applications have significantly reduced cost, lowered risk and improved performance. However, there is still huge potential for even greater benefits from expanded application of HEC in aerospace and it is timely to look at what significant advances in simulation can be initiated now. Here we explore four challenging and potentially fruitful areas for advancement.

The first challenge is Digital Flight that simulates aircraft dynamic flight and advances the application of CFD to broader areas of the flight envelope. The second challenge is space vehicle Launch Simulation in which high-fidelity modeling of the mission profile is used to improve mission planning and design as well as provide better assessments of risk. The third challenge is Liquid Rocket Engine Fuel System Simulation that exemplifies the use of high-fidelity modeling of complex systems for development of space trans-